6086 *Macromolecules* **2009**, *42*, 6086–6097
DOI: 10.1021/ma900530j

Macromolecules
ARTICLE

Cutinase-Catalyzed Deacetylation of Poly(vinyl acetate)

Åsa M. Ronkvist, Wenhua Lu, David Feder, and Richard A. Gross*

NSF I/URC for Biocatalysis and Bioprocessing of Macromolecules, Department of Chemical and Biololgical Sciences, Polytechnic University, Six Metrotech Center, Brooklyn, New York 11201

Received March 11, 2009; Revised Manuscript Received July 3, 2009

ABSTRACT: Poly(vinyl acetate), PVAc, is an industrially important polymer used in adhesives, textile fibers, paper products and coating materials. This paper reports catalytic activities of cutinases from *Humicola insolens* (HiC), *Pseudomonas mendocina* (PmC), and *Fusarium solani* for PVAc hydrolysis. PVAc was distributed as thin films throughout highly porous styrene divinyl benzene beads with known surface area. Cutinase activity for PVAc deacetylation was assayed using a pH-stat to measure NaOH consumption versus time and PVAc concentration was expressed as square meter per milliliter. HiC had maximum initial activity at 70 °C whereas PmC and FsC performed best at 50 and 40 °C, respectively. To limit background chemical hydrolysis, kinetic studies for all three cutinases were performed at pH 7.5. Initial activities for each cutinase at their optimal reaction temperatures were fit by the Michaelis−Menten kinetic model. PmC had the highest affinity for PVAc with K_m of 20 $m^2 \cdot mL^{-1}$. Furthermore, HiC and FsC had the highest and lowest catalytic efficiency values, 102 and 20 $L \cdot h^{-1} \cdot m^{-2}$, respectively. Study of cutinase stability showed that, within 96 h at 40 °C, FsC lost 93% of its initial activity. In contrast, incubations of HiC and PmC retained 67 and 47% of their activities during incubations for 192 h at 70 and 50 °C, respectively. For HiC, % yields of water-soluble copolymer after incubations for 144 and 192 h are 13 and 14%, respectively. The mol % of VAc in P(VAc-*co*-VOH), solubilized during incubations for 24, 144, and 192 h, is 30, 19, and 6%, respectively. Thus, HiC can deacetylate PVAc to high extents. At 24 h, where P(VAc-*co*-70 mol %VOH) was isolated from the aqueous phase, the sequence distribution along chains determined by ^{1}H NMR was found to be highly blocky ($\eta = 0.36 \pm 0.06$).

Introduction

Polymers comprising vinyl acetate (PVAc) and vinyl alcohol (PVOH) are of major industrial importance. Traditional uses are as components in adhesives, textile fibers, paper products and coating materials.[1,2] They also have been incorporated into biodegradable materials. For example, poly(lactic acid), poly(ε-caprolactone), and poly(hydroxybutyrate) were blended with PVAc, PVOH, or with their copolymer P(VAc-VOH), in order to improve corresponding material mechanical properties or to control degradation rates.[3−6] Furthermore, hydroxyl groups on PVOH can be modified to attach growth factors, adhesion proteins or other molecules of biological importance. Since PVOH is generally considered to be biocompatible, such polymers are of great interest for hydrogel scaffolds in tissue engineering.[6,7] PVAc, combined with PVOH, has also been studied for applications in drug release systems, such as sustained release coatings, matrix pellets, and drug carriers.[8,9]

PVOH and P(VAc-VOH) of various compositions are commercially produced through saponification of PVAc. This is a consequence of the fact that vinyl alcohol readily tautomerizes.[10] PVAc is a water insoluble polymer, whereas PVOH is water-soluble. As the deacetylation of PVAc progresses, the formation of partially hydrolyzed P(VAc-*co*-VOH) will, at a certain point, become water-soluble. Identification, study and development of enzymes with activity for PVAc deacetylation have the potential to be mild and selective, whereas traditional chemical methods require either strong basic or acidic environments. Enzyme-catalyzed routes to deacetylate PVAc can be of great value to recycling industries, since it would facilitate removal of adhesives and coatings which tend to agglomerate during recycling processes, resulting in poor paper quality and significant machine downtime.[1] Furthermore, enzymatic deacetylation can be used to increase the hydrophilicity of polymeric surfaces that contain vinyl acetate units in homo- or copolymers. Enhanced hydrophilicity by increase in the concentration of hydroxyl groups at surfaces is valuable to improve water permeability and apply color agents or various coatings.[2,6,11] In contrast to alkaline surface treatments, enzyme-catalyzed hydrolysis accesses only material surfaces due to its large size and incompatibility with polymeric substrates. This has the potential to provide large changes in surface functionality while not affecting bulk properties.[11]

Fungal organisms produce extracellular enzymes called cutinases. Their natural function is to catalyze hydrolysis of cutin ester bonds. Cutin is a lipid polyester found in the cuticle of higher plants and serves as an armor protecting these organisms from microbial attack.[12−14] Thus, organisms that excrete cutinases have a distinct advantage in gaining entry into plant leaves leading to further attack on plant systems. Cutinases are the smallest members of the serine α/β hydrolase superfamily, with molecular weights about 20 K.[15] The best studied cutinase is a 22 kDa enzyme from the fungus *Fusarium solani*.[16−18] Its three-dimensional structure has been solved to 1.0 Å resolution.[15] The cutinase structure has been related to its activity[15,19] the active site consists of the catalytic triad Ser120, Asp 175, and His188. However, unlike most lipases, the catalytic serine is not buried under an amphipathic loop but is accessible to the solvent. Apart from hydrolyzing cutin ester bonds, cutinases have been reported to have hydrolytic activity on a variety of synthetic polyesters and polyamides.[11,20−26]

Interestingly, Borch et al.[1] were first to discover that cutinase, most notably that from *Humicola insolens* (HiC), is active for PVAc deacetylation. They compared the activity of three different thermostable variants of purified HiC for PVAc emulsion hydrolysis.[1] This biotransformation is fascinating since it requires

*Corresponding author.

 Published on Web 07/20/2009

that cutinases have an active site that is sufficiently open to allow access of esters linked to bulky chains by secondary hydroxyl groups. Initial interest in cutinase-catalyzed PVAc hydrolysis was focused on reducing the problem of agglomerated PVAc residues, so-called stickies, in paper recycling processes. Borch et al.[1] claimed that a relatively small degree of hydrolysis (4−10%) was sufficient to largely eliminate stickies from paper. They determined the degree of hydrolysis by measuring acetate release using capillary electrophoresis after a 10 min incubation time and quantified the deposition of agglomerates on a metal surface by mass uptake after 18 h using a tensiometer. Thus, no kinetic data was provided and the substrate and products formed were poorly defined. Later Matamá et al.[2] and Silva et al.[25,27] reported that an acrylic fiber containing 7% of vinyl acetate as comonomer was modified by a culture broth containing *F. solani* cutinase (FsC) with a purity range of 50−70%. The degree of hydrolysis was studied by staining liberated hydroxyl groups and evaluating the color strength. However, they did not detect the coproduct acetic acid due to an assay method that lacked sufficient sensitivity.[2] Chahinian et al.[28] compared the kinetic behavior of FSC using aqueous solutions and emulsions of vinyl acetate with that of different esterases and lipases. While esterases expressed maximum activity in the soluble concentration range, cutinase displayed maximum activity for emulsified vinyl acetate.

This paper reports a detailed study and comparison of the catalytic activities of cutinases from three different organisms, using PVAc as the model substrate. This is the first paper describing how different cutinases perform relative to each other for a specific activity. Previous papers,[1,2,25,27,28] largely due to the lack of commercially available cutinases, compared one cutinase to other enzyme families. Cutinases included in this study are from *H. insolens* (HiC), *Pseudomonas mendocina* (PmC), and *F. solani* (FsC). These cutinases were first purified (>95%) and are quantified in mol/mL rather than by units, which was previously done by others that used impure enzymes from culture broths.[2,25,27,28] Heuman et al.[22] showed that units based on a surrogate assay may poorly correlate to the activity for the substrate of study. Furthermore, in previous studies of PVAc enzymatic hydrolysis,[1,2,25,27] the actual PVAc surface accessible to cutinases was not known. Thus, these workers had a large part of PVAc (the bulk) that was not available to the enzyme, thereby reducing the observed degree of hydrolysis. Without knowledge of surface area accessible to the cutinase, it is difficult to deduce if a low degree of hydrolysis is caused by a large bulk fraction or due to low enzyme activity. Furthermore, a method is reported herein whereby PVAc was distributed throughout highly porous styrene divinyl benzene beads with known surface area. The PVAc distribution and access of the cutinase to PVAc were assessed by infrared microscopy imaging. Knowledge of accessible substrate surface area substrate allowed for the first kinetic investigation of enzyme-catalyzed PVAc hydrolysis.

Kinetic studies of PVAc enzymatic hydrolysis were determined by a pH stat that provided online measurements. For each cutinase, optimal temperature and pH values for PVAc were determined and the hydrolysis rates were fitted to known kinetic models. In addition to initial kinetic values, stability of cutinases during long-term incubations with PVAc was studied. An advantage of using a pH-stat is that it monitors the total amount of liberated acetate due to cutinase catalyzed PVAc hydrolysis without taking into account the origin of the release, whether it is from the hydrolysis of water-insoluble PVAc or from formed water-soluble P(VAc-*co*-VOH). The extent that cutinases catalyzed PVAc hydrolysis was also determined by measuring weight loss of PVAc coated beads. Results obtained from weight loss measurements were correlated to the degree of hydrolysis of formed water-soluble poly(VAc-*co*-VOH), determined by proton (^{1}H) NMR. Moreover, the sequence distribution of the formed water-soluble poly(VAc-*co*-VOH) was evaluated by ^{1}H NMR to determine the selective properties of cutinases.

Materials and Methods

Materials. HiC and PmC were kind gifts from Novozymes (Bagsvaerd, Denmark) and Genencor (Danisco US Inc., Genencor Division, Palo Alto, CA), respectively. Wild-type FsC cloned into *Pichia pastoris* was purchased from DNA 2.0 (Menlo Park, CA). Methods for fermentative synthesis and purification of FsC are described below as are methods for purification of HiC and PmC. Butyl sepharose 4 fast flow was obtained from GE Healthcare Bio-Sciences Co. PVAc with weight average molecular weight (M_w) 13 000 was obtained from Sigma-Aldrich (430439). Macroporous styrene-divinylbenzene beads (S-DVB), commercially known as Amberlite XAD1180, was a kind gift from Rohm & Haas/Ion Exchange Resins (Philadelphia, PA). All other chemicals were purchased from Sigma-Aldrich Co in the highest available purity and were used without further purification.

High Density Cell Culture and Expression of FsC. The method is a modification of that previously published by Tolner et al.[29] Precultures were performed in a shaker-incubator (innova 4900, New Brunswick Scientific Co.) at 200 rpm, 28 °C, with 0.5 mL of *P. pastoris* strain DP91 from glycerol stock in 50 mL BMGY medium consisting of the following (g/L): yeast extract, 10; peptone, 20; yeast nitrogen base without amino acids and ammonium sulfate, 3.4; glycerol, 10; ammonium sulfate, 10; biotin, 4×10^{-4}; histidine, 0.026; 100 mM potassium phosphate, 1 L for 20 h. Cells were collected by centrifuge at 6000 rpm for 10 min and resuspended in a basal salts medium (BSM, 20 mL) consisting of (g/L): phosphoric acid, 85%, 26.7 mL; calcium sulfate, 0.93; potassium sulfate, 18.2; magnesium sulfate−$7H_2O$, 14.9; potassium hydroxide, 4.13; glycerol, 40 as seeds for inoculation of fermentation.

Fermentations were performed in a 7.5 L fermentor (Bio110, New Brunswick Scientific Co.) with control of agitation, dissolved oxygen (DO), temperature and pH. BSM medium was used as fermentation medium with addition of 12 mL/L of filter sterilized PTM1 trace salts solution (g/L): cupric sulfate-5 H2O, 6; sodium iodide, 0.08; manganese sulfate−-H_2O, 3.0; sodium molybdate−$2H_2O$, 0.2; boric acid, 0.02; cobalt chloride, 0.5; zinc chloride, 20; ferrous sulfate−$7H_2O$, 65; biotin, 0.2; sulfuric acid, 5 mL. The medium pH was adjusted to 5.0 by addition of 28% (w/w) ammonium hydroxide before inoculation. Seeds were inoculated at 10% to fermentor containing 3.5 L of BSM medium. Initial cell density (OD600 nm) was about 2.0−3.0. Temperature and aeration were set at 28 °C and 1.5 vvm, respectively. The pH was controlled at 5.0 by feedback-response controlled addition of 28% ammonium hydroxide or 30% phosphoric acid solution. The DO was maintained at 40% of air saturation by automatic adjustment of agitation speed. When glycerol was exhausted, which was indicated by a DO spike, a glycerol fed-batch phase was initiated by addition of 50% (w/w) glycerol with 12 mL/L PTM1 trace salts solution at a rate of 18 mL/L/h for 6 h. Expression of cutinase was induced by addition of methanol when glycerol exhausted again after glycerol fed-batch phase. Pure methanol with addition of 12 mL/L PTM1 trace salts solution was fed at a rate of 5 mL/L/h for 80 h. To limit foaming, antifoam 204 was added when necessary.

Cutinase Purification. Cell culture was centrifuged (Allegra-TM 25 R, Beckman Coulter) at 8000 rpm, 4 °C for 30 min. The resulting supernatant containing FsC cutinase was enriched to ~100 mL by ultrafiltration using PelliconTM-2 TFF system (Millipore) with 10 KD cassette filters (Biomax10 membrane, Millipore). Then, FsC was purified by fast perfusion liquid chromatography (FPLC). A six-His tag at the N-terminus of FsC allowed purification by a metal chelating affinity column. The purification was performed on a VISION Workstation (Applied Biosystems Co.) with a 16 mm/100 mm (D:L) POROS MC 20 μm

column (Applied Biosystems Co.) at a flow rate of 40 mL/min. Column metal sites were presaturated by 100 mM $NiCl_2$ solution. Buffer (NaH_2PO_4, 50 mM) with 0.5 mM imidazole (pH 8.0) and 50 mM NaH_2PO_4 buffer with 100 mM imidazole (pH 8.0) were used as starting buffer and elution buffer, respectively. Impurities uncombined with metal in column were removed by washing with two column volumes (CV) of the starting buffer, and then FsC was eluted using an imidazole gradient from 0.5 to 100 mM by mixing the starting buffer with elution buffer. The peak fractions related to FsC in gradient step (from 0.8 CV to 2.5 CV) were collected and desalted (see below).

PmC was purified by hydrophobic interaction chromatography. The purification was performed in a 1.5 mm/500 mm (D:L) econo column (Biorad) with a butyl sepharose support. Hepes buffer (20 mM) with 1.5 M NaCl (pH 8.0) was used as starting buffer. Impurities uncombined with support in column were removed by washing with 5 CV of the starting buffer, and then PmC was eluted by adding 5 CV of 20 mM hepes buffer (pH 8.0). The fractions related to PmC were collected and desalted.

The collected and purified FsC and PmC fractions, as well as the received HiC, were each desalted using an ultrafiltration unit (Milcon, Millipore) with a 10 kDa ultrafiltration membrane (YM10, Millipore). FsC and HiC were desalted using distilled water, whereas PmC was desalted in a 30% glycerol solution to avoid aggregation and subsequent precipitation. FsC and HiC solutions were then lyophilized, and thereafter, they were dissolved in 30% glycerol at a similar concentration as PmC. The importance of glycerol to improve cutinase stability and activity is discussed below.

Quantification of Cutinase Concentration and Purity. Purified enzyme solutions were analyzed on an Experion TM 260 (Biorad) microfluidic gel-based electrophoresis system. This analysis provided quantification of cutinase molecular weight, concentration and purity. Each cutinase was run in triplicate.

Coating of PVAc within a Macroporous Resin. A method was developed to coat PVAc within Amberlite XAD1180, a macroporous styrene−devinylbenzene (S-DVB) resin. These beads have a surface area of 450 m^2/g and a pore diameter distribution of 30−50 nm. PVAc (20 g), dissolved in 200 mL chloroform, was mixed with 15 g Amberlite XAD1180 in a 500 mL round-bottom flask. The chloroform was evaporated by mounting the flask onto a roto evaporator without vacuum, placing the flask in an external water bath at 40 °C and rotating the flask at 150 rot/min until the coated beads were visibly dry (approximately 48 h). Thereafter, the beads were further dried overnight in a vacuum oven (40 °C, 30 mmHg) to remove residual solvent. Assuming PVAc is uniformly covered throughout the internal bead surface area, PVAc distribution is 2 mg/m^2 and the mean PVAc thickness is approximately 2 nm. Furthermore, PVAc within S-DVB resin accounts for 43%-by-wt of the resulting coated beads.

Imaging PVAc Distribution and Enzymatic Access to Substrate by Infrared (IR) Microspectroscopy. The method was adapted from that described elsewhere.[30,31] IR microspectroscopy was performed with a Spotlight FTIR spectrometer (Perkin-Elmer). The coated beads were embedded in paraffin wax and the blocks were sectioned at a thickness of 10 μm using a stainless steel blade on a cryomicrotome (IEC). Sections were coated on BaF_2 disks and placed in a standard FTIR slide mount for data collection. Spectra were collected in the transmission mode from 4000 to 750 cm^{-1} with 128 scans per point and 4 cm^{-1} resolution. The peak areas of A (1667−1776 cm^{-1}) and B (1430−1500 cm^{-1}) are proportional to relative quantities of PVAc and S-DVB, respectively. Access of cutinase to PVAc within macroporous beads was assessed by comparing intensities of O−H stretching vibrational bands (3300−3700 cm^{-1}) relative to bands corresponding to S-DVB.

Cutinase-Catalyzed Deacetylation of PVAc Monitored by pH-stat. Cutinase activity for PVAc deacetylation was assayed using a pH-stat apparatus (Titrando 842, Metrohm) equipped with Tiamo 1.1 software. All PVAc deacetylation reactions were performed in 0.5 mM Tris−HCl buffer with 10% glycerol. The low buffer concentration stabilized the initial pH that would otherwise fluctuate due to solubilization of atmospheric carbon dioxide.[32] For all pH stat assays, the PVAc concentration was expressed as m^2/mL. Initial deacetylation rates were expressed as units of micromoles of added NaOH per hour and milliliters of reaction volume. Studies of enzyme activity on PVAc in pH-stat experiments were performed over temperatures from 30 to 90 °C, pH values 6.5 to 9.0, cutinase concentrations 0 to 30 nmol/mL, and PVAc concentrations 0 to 60 m^2/mL. All reactions were performed in duplicates. Control samples (without enzyme) were run for each parameter in order to determine background chemical hydrolysis that was subtracted from total hydrolysis to measure enzyme-catalyzed PVAc deacetylation.

Cutinase Thermo Stability Measurements. Stock solutions (50 mL) of 0.5 mM Tris−HCl buffer with 10% glycerol at pH 7.5 and 15 nmol/mL of either HiC, PmC or FsC were placed in oil baths at 70, 50, and 40 °C, respectively. At different time points from 0 to 192 h, 3 mL aliquots were withdrawn from stock solutions incubated at selected temperatures. These aliquots were added to separate vials containing 150 mg of PVAc coated beads. Initial rates of PVAc deacetylation at each incubation time point were measured using the pH-stat as described above at 70, 50, or 40 °C for HiC, PmC, and FsC, respectively. Percent losses in activity were determined from the relative ratio of measured initial PVAc deacetylation rate to the initial rate at time 0 h.

Degradation Studies. PVAc coated S-DVB beads (700 mg of which 300 mg is PVAc) were placed in vials containing 6 mL of 1 M Tris−HCl buffer (pH 7.5) with 10% glycerol and 90 nmol of a cutinase. Time course studies (0 to 192 h) were performed by placing vials in a rotary shaker-incubator at 100 rpm, from 0 to 192 h, at optimal temperature values determined from pH-stat experiments (see above). At sampling times, three replicate vials for each cutinase were removed from the shaker-incubator, beads were separated from the aqueous media by filtration using Vacmaster-10 (Biotage) with isolute columns having a frit porosity of 20 μm. Filtrates were collected and saved for ^{1}H NMR analysis (see below). The beads were washed extensively with distilled water, dried in vacuo (30 mmHg) for 48 h at 40 °C and then weighed. Weight loss was calculated by subtracting the measured final weight from the initial weight. Control samples (without enzymes) were also carried out in triplicate in order to account for potential contribution to weight loss by chemical hydrolysis. Final weight loss values due to cutinase-catalyzed hydrolysis were calculated by subtracting background weight loss attributed to chemical hydrolysis.

Proton Nuclear Magnetic Resonance (^{1}H NMR). Incubation media collected as filtrates from degradation studies was analyzed by ^{1}H NMR to determine if water-soluble P(VAc-*co*-VOH) was formed and, if so, what degree of hydrolysis occurred. Prior to ^{1}H NMR analysis, buffer and glycerol were removed from incubation media by ultrafiltration (Millipore Stirred Cell Model 8400, 400 mL) using a membrane with a 1K molecular weight cutoff and washing the retentate three times with 250 mL portions of distilled water. The resulting retentate solution was freeze-dried to remove water and to obtain the copolymer in solid form. ^{1}H NMR spectra were recorded on a Bruker AVANCE 300 spectrometer. Chemical shifts reported were referenced to internal tetramethylsilane (0.00 ppm) or to the solvent resonance at the appropriate frequency. The sample concentration was 3% w/v in DSMO-d_6. Instrument parameters for ^{1}H NMR experiments were as follows: 3.4 s acquisition time, spectral width 4800 Hz, 32 000 data points, relaxation delay 10 s, and 64 transients.

Results and Discussion

Quantification of Cutinase Concentration and Purity. Solutions of HiC, PmC, and FsC, purified as described in the Materials and Methods section, were analyzed by an Experion microfluidic gel-based separation system. Proteins are

visualized by laser-induced fluorescence detection. Addition to samples of fluorescent dye and two internal markers enabled analysis of protein molecular weight and concentration.[33] The results are shown in Figure 1 as a virtual gel. HiC (lane 1−3) and FsC (lane 7 and 9) are enzymes of similar size (23.1 ± 0.2 and 22.6 ± 0.2 kDa, respectively) whereas PmC (lane 4−6) is 30.0 ± 0.1 kDa. These values of molecular weight are in good agreement with those in the literature.[17,34−36] By comparing the peak area of cutinases in the electropherogram to the upper alignment marker at 260 kDa proteins, enzyme concentrations were determined. Stock solutions of HiC, PmC, and FsC had concentrations of 1.5 ± 0.2, 1.9 ± 0.1, and 1.9 ± 0.1 mg/mL, respectively. Furthermore the purities of these proteins are 97 ± 0.4%, 99 ± 0.2% and 96 ± 2% respectively. On the basis of a prior report by Matamá et al.,[2] who showed that glycerol improves the stability of FsC, cutinases studied herein were also stored in a mixture of distilled water and glycerol. Further study of glycerol with HiC and PmC in our laboratory showed it was similarly useful for these cutinases.

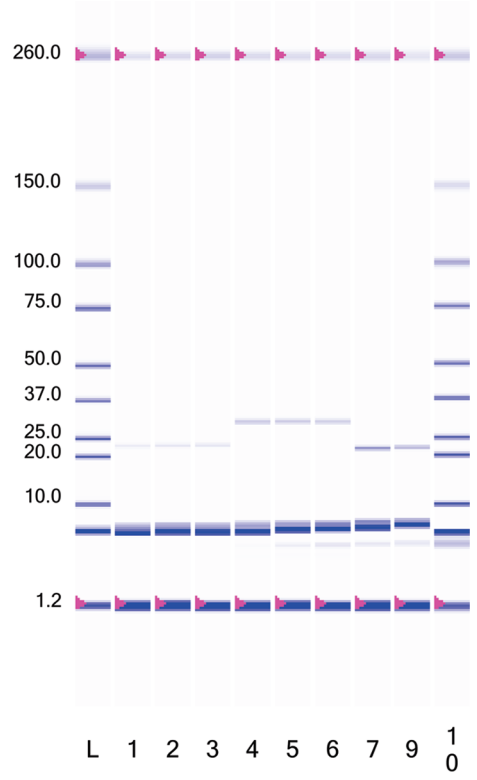

Figure 1. Virtual gel by experion of purified HiC (lanes 1−3), PmC (lanes 4−6) and FsC (lanes 7 and 9) and the ladder with proteins of size 10−260 kDa (lane L and 10).

It is common to dose cutinase according to its activity for release of *p*-nitrophenol (pNP) from pNP esters of short chain fatty acids. Subsequently, based on the activity of cutinases on these model substrates, their activities were compared for polymer hydrolysis reactions.[2,20,22,27] However, Heumann et al.[22] showed there was no correlation between cutinase activity on *p*NP esters and their activity for hydrolysis of poly(ethylene terephthalate), PET. Therefore, rather than quantifying enzymes by units, we opted to provide nanomol per milliliter of purified cutinases used in a given biotransformation.

Imaging of PVAc Distribution and Enzymatic Access by IR Microspectroscopy. To increase the surface area of PVAc and provide ease of handling for what would normally be a sticky substrate, PVAc was coated within Amberlite XAD1180, a macroporous styrene-devinylbenzene (S-DVB) resin. Amberlite XAD1180 has a surface area of 450 m^2/g and a pore diameter distribution of 30−50 nm. IR microspectroscopy was used to probe PVAc distribution within S-DVB macroporous resin. The IR spectrum of pure PVAc showed a characteristic vibrational stretching absorption band corresponding to ester carbonyl groups at 1738 cm^{-1}.[37] In contrast, the IR spectrum of S-DVB is dominated by aromatic C−C stretching centered at 1465 cm^{-1}.[30] Exploiting these spectral differences between PVAc and the bead matrix, we obtained an IR image showing PVAc distribution within beads (Figure 2). The IR image shows PVAc is spread throughout the entire internal bead surface area with nearly uniform coverage. The PVAc coating was prepared using a weight ratio of PVAc to S-DVB of 0.75 g/g. Using the minimum surface area of S-DVB according to its product datasheet, average PVAc coverage is 2 mg/m^2. Assuming the PVAc coating is uniform throughout internal bead surfaces, the mean PVAc thickness is approximately 2 nm. Furthermore, the coating would be sufficiently thin to enable cutinases to diffuse throughout S-DVB beads since their pore diameter is 30−50 nm and the cutinases have sizes < 5 nm.[38]

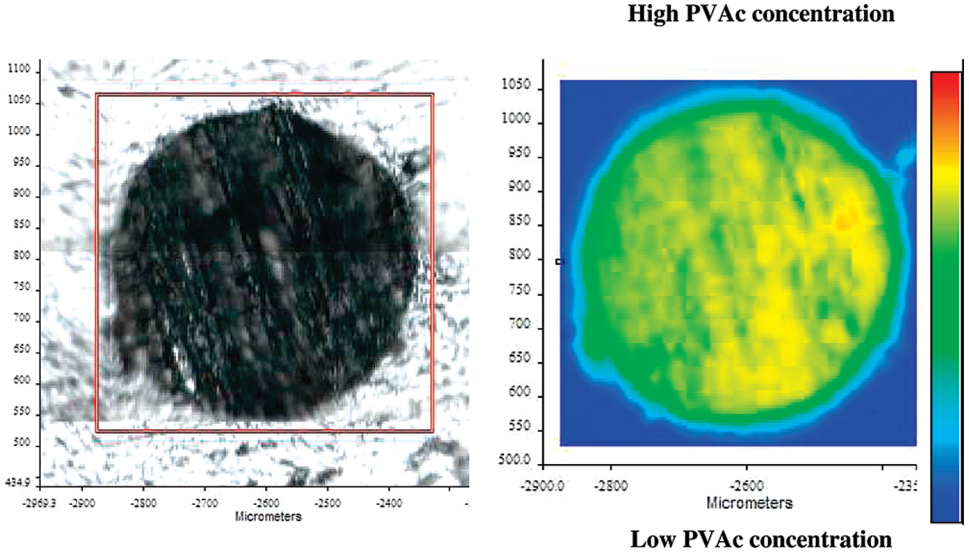

Figure 2. Visible light image (left) of the PVAc coated S-DVB bead embedded in paraffin and cross-sectioned at 10 μm thickness. The red box indicates the area imaged by the IR microscope. The right panel shows the PVAc distribution throughout the center section of the PVAc coated bead.

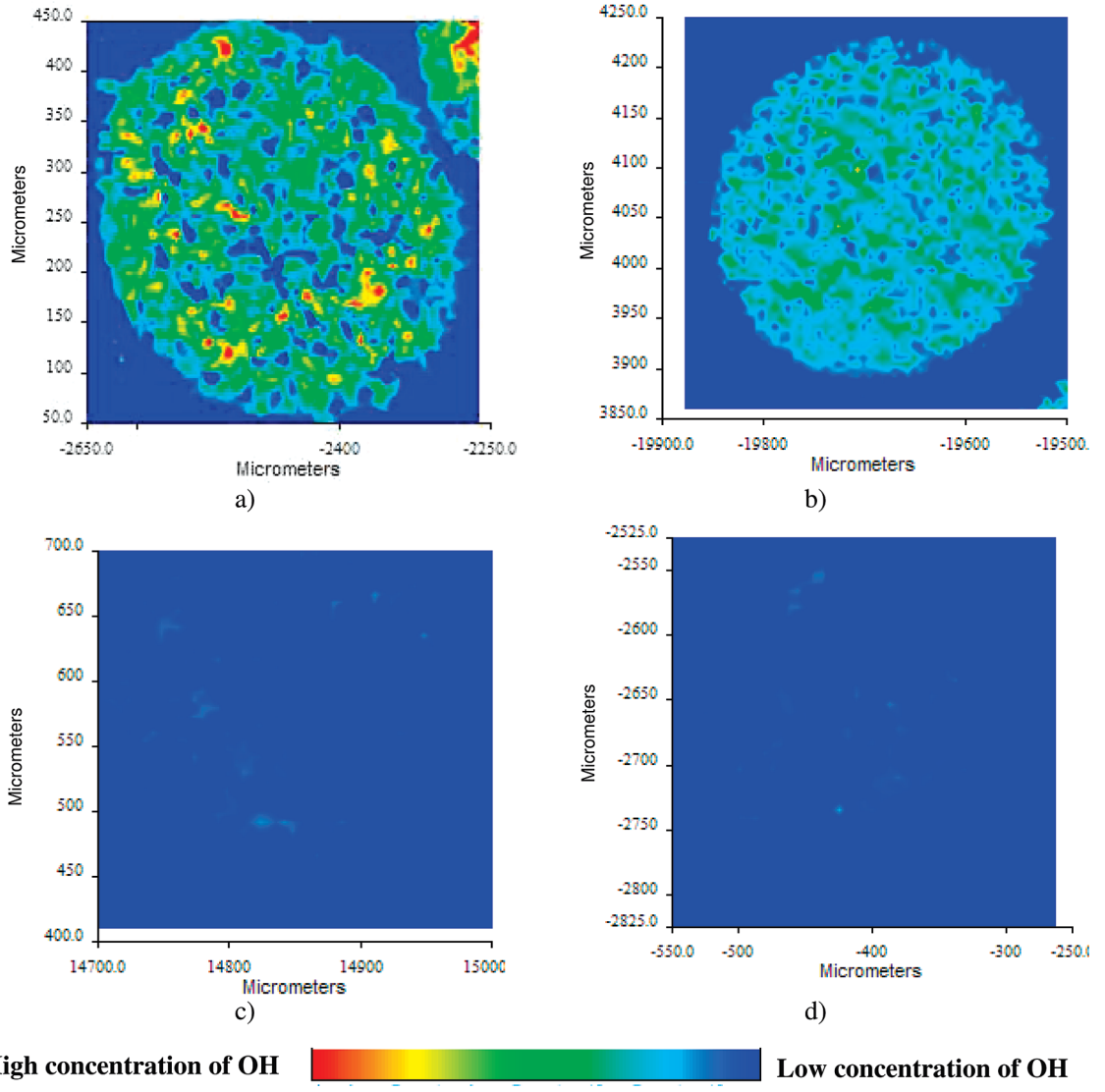

Figure 3. Infrared microspectroscopy images to analyze hydroxyl group distribution within a series of PVAc coated S-DVB beads exposed 15 h to 0.5 mM Tris buffer with 10% glycerol in pH 7.5 with either 1.6 nmol/mL of (a) HiC at 70 °C, (b) PmC at 50 °C, (c) FsC at 40 °C, or (d) no cutinase at 70 °C (control).

Access of cutinase to PVAc within macroporous beads was assessed by determining the corresponding distribution of hydroxyl groups both before and after incubation with cutinases. In other words, if cutinases have access to PVAc throughout beads and are active for PVAc deacetylation, then a uniform increase in concentration of hydroxyl groups all through beads will be observed. Increase in hydroxyl concentration was determined by measuring O−H stretching vibrational absorptions at 3300−3700 cm^{-1} and comparing them to aromatic C−C stretching bands, centered at 1465 cm^{-1}, corresponding to S-DVB. Figures 3 a to d illustrate the distribution of hydroxyl groups within PVAc coated S-DVB beads after 15 h exposures to either (a) HiC at 70 °C, (b) PmC at 50 °C, or (c) FsC at 40 °C or to (d) no enzyme at 70 °C (control) in 0.5 mM Tris buffer with 10% glycerol at pH 7.5. Incubation temperatures are based on results from temperature−activity relationship studies described below (see also Figure 4a). HiC and PmC exposed PVAc/S-DVB samples illustrated in Figure 3, parts a and b, respectively, shows a higher content of hydroxyl groups than the control sample (Figure 3d) and the distribution of the hydroxyl groups is throughout PVAc coated beads. This indicates that the cutinases diffuse within beads and can access all PVAc covered surfaces. Given these results, and that S-DVB beads (Amberlite XAD1180) have a surface area of 450 m^2/g (see Materials and Methods section), the PVAc concentration available for cutinase-catalyzed hydrolysis can also be expressed as square meter per milliliter. In contrast to results above using HiC and PmC, FsC-exposed PVAc-coated beads display a similar hydroxyl group distribution as the control sample (Figure 3, parts c and d, respectively). This is due to FsC deactivation during long-term incubations (see relevant discussion below).

Effect of Temperature and pH for Cutinase Deacetylation of PVAc. Cutinase activity for PVAc deacetylation was assayed using a pH-stat to measure NaOH consumption versus time. Titration of NaOH by the pH stat keeps the pH constant as acetate is liberated due to cutinase-catalyzed PVAc hydrolysis. Initial slopes in μmol NaOH titrated per hour and reaction volume were recorded by the pH-stat during the first hour of incubations, and these slope values were used in subsequent plots to assess cutinase activity as a function of incubation parameters (e.g., temperature, pH). Typical plots of NaOH titrated versus time are given in the Supporting Information (Figure S-1). Normally, slopes were measured for lines generated between 15 and 30 min with

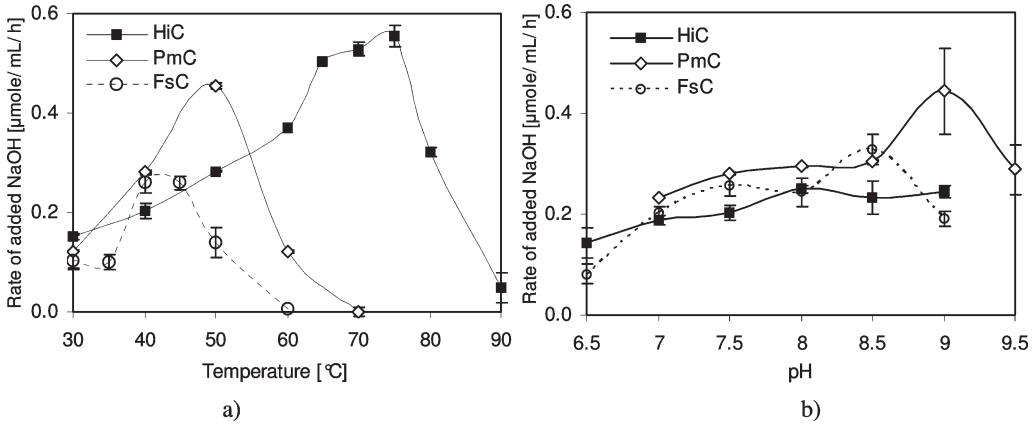

Figure 4. Activity of cutinases for PVAc hydrolysis determined using a pH-stat, 10 mM NaOH as titrant, 8 m^2/mL PVAc, and 0.5 nmol/mL of cutinase in 8 mL of 0.5 mM Tris buffer containing 10% glycerol. Figure 4a displays temperature dependence at pH 7.5 whereas Figure 4b displays pH dependence at 40 °C. Error bars represent a standard deviation method based on duplicate repeats.

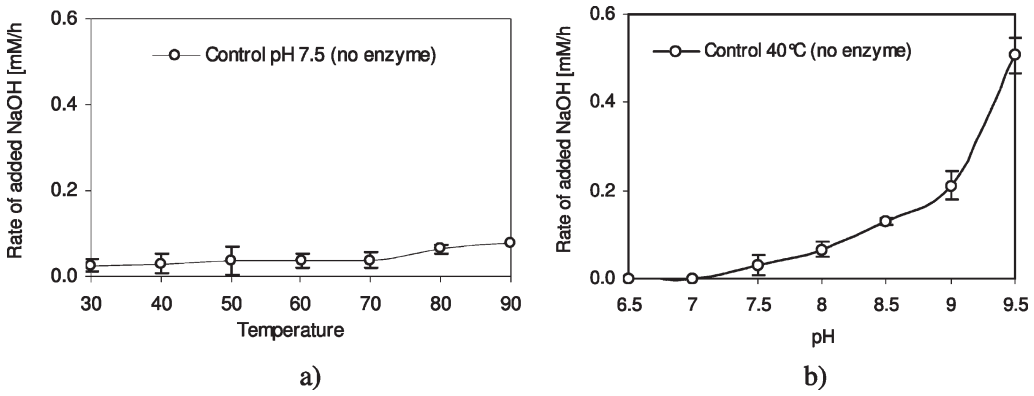

Figure 5. Chemical hydrolysis of PVAc in control experiments determined using a pH-stat, 10 mM NaOH as titrant, 8 m^2/mL PVAc, and no cutinase in 8 mL of 0.5 mM Tris buffer containing 10% glycerol.Part a displays how temperature influences events of chemical hydrolysis at pH 7.5 whereas part b displays pH dependence at 40 °C. Error bars represent standard deviation method based on duplicate repeats.

linear regression (R^2) values ≥0.97. Figure 4a shows the effect of temperature on cutinase initial activity at pH 7.5, and Figure 4b illustrates the effect of pH on the cutinases at 40 °C. For HiC, temperature has a significant effect on its activity while pH does not. As the temperature increases from 30 to 75 °C, HiC activity increases almost 4-fold. Maximum HiC activity (0.50−0.56 μmol/(mL/h)) occurs from 65 to 75 °C. Thereafter, HiC activity drops steeply at 90 °C, likely due to thermal induced denaturation. In contrast, HiC activity varied little, from 0.20 to 0.24 μmol/(mL/h), over a pH range 6.5 to 9.0 (Figure 4b).

Thermal stabilities of PmC and FsC were lower than that observed for HiC. PmC and FsC reach their maximum activities of 0.45 and 0.26 μmol/(mL/h) at 50 and 45 °C, respectively (Figure 4a). At temperatures above 50 °C, both enzymes are deactivated. Similar maximum activities of PmC and FsC are reached in the pH study; 0.45 and 0.33 μmol/(mL/h) at pH 9.0 and 8.5, respectively. Optimal temperature and pH values for FsC determined here, based on PVAc hydrolysis, are in agreement with previous literature reports where acrylic−vinyl acetate[2] and triglycerides[39] were used as substrates.

It is understood that some applications of cutinases may restrict the pH and temperature at which they are used. Since this is not a limitation in this work, studies described below with HiC, PmC, and FsC were conducted at pH and temperature values that both limit background chemical hydrolysis while supporting optimal cutinase activity. Figure 5a shows that, even at temperatures up to 80 °C at pH 7.5, no enzyme control experiments show PVAc hydrolysis remains low (∼ 0.06 μmol/(mL/h) NaOH). Thus, experiments performed below with HiC, PmC and FsC are performed at their experimentally determined optimal temperatures (70, 50, and 40 °C, respectively). In contrast, control experiments at 40 °C show that, at pH values above 8.0, rates of PVAc chemical hydrolysis become significant (Figure 5b). Hence, even though PmC and FsC have optimal activities at pH 9.0 and 8.5, respectively, experiments with PmC, FsC, and HiC are all performed at pH 7.5.

Kinetics. The pH-stat assay was used to determine the dependence of PVAc hydrolysis rate on cutinase concentration. Concentrations of the three cutinases were varied at fixed PVAc surface concentration (20 m^2/mL) in 3 mL of 0.5 mM Tris−HCl buffer with 10% glycerol, at pH 7.5, for one hour, at 70, 50, and 40 °C for HiC, PmC and FsC, respectively. Experimental rates of enzymatic deacetylation, determined from linear slopes of NaOH vs time data (see Figure S-2, Supporting Information), are displayed as filled markers in Figure 6. A linear dependence of NaOH consumption rate with increased cutinase concentration was obtained up to 1.0, 2.0, and 4.3 nmol/mL for HiC, PmC, and FsC, respectively (Figure 6, parts a, b, and c, respectively). Thereafter, the rate levels off as cutinase concentration was increased due to limitations in substrate concentration. In other words, as the cutinase concentration increases, eventually it reaches a point where the amount of

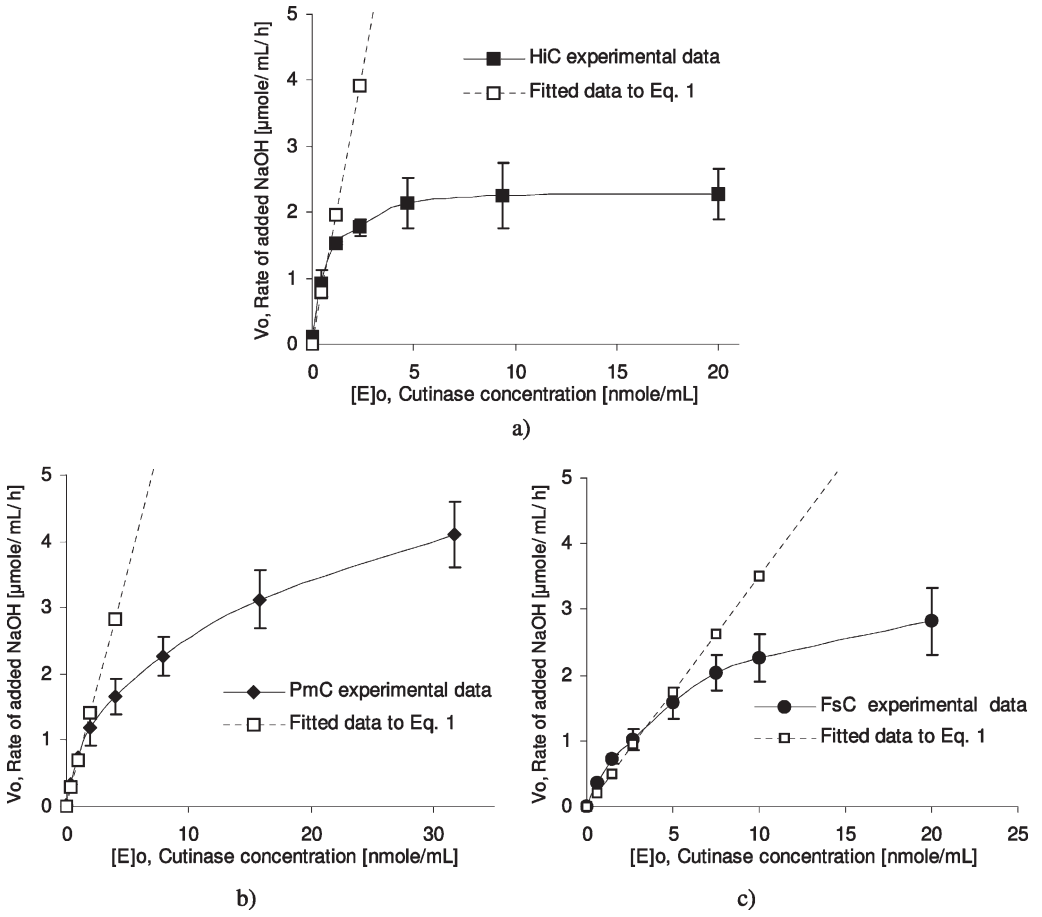

Figure 6. Initial rate of NaOH consumption as a function of cutinase concentration, at fixed PVAc concentration (20 m^2/ml) for (a) HiC at 70 °C, (b) PmC at 50 °C, and (c) FsC at 40 °C. Experimental values are plotted as filled squares and solid lines, whereas dotted lines are fitted to eq 1. Error bars represent standard deviation method based on duplicate repeats.

substrate becomes limiting, and as it is kept to a constant value. The result is that the rate asymptotically approaches a maximum.

In the classical kinetic model of Michaelis−Menten (M−M), the initial reaction rate (V_0) is expressed as function of substrate concentration $[S]_0$:

$$V_0 = \frac{V_{max}[S]_0}{K_m + [S]_0} \quad (1)$$

Here

$$V_{max} = k_{cat}[E]_0 \quad (2)$$

and K_m is the Michaelis constant, V_{max} is the maximal reaction rate, and k_{cat} is the turnover number. Since V_{max} is proportional to $[E]_0$ (eq 2), there is a linear relationship between V_0 and $[E]_0$. The M−M model is therefore only applicable when $[S]_0$ is in excess.[40,41] Results in Figure 6 show that for HiC, PmC, and FsC, $[E]_0$ values of 1.0, 2.0, and 4.3 nmol/mL, respectively, give maximum hydrolysis rates in the linear region. These concentrations were then used to determine initial hydrolysis rates as function of substrate concentration (see Figure 7).

A linearized expression of the M−M eq 1 is the Lineweaver−Burk equation:

$$\frac{1}{V_0} = \frac{1}{V_{max}} + \frac{K_m}{V_{max}[S]_0} \quad (3)$$

Here V_{max} and K_m are determined from the slope and y-intercept of the linear regression line. The experimental relation between initial deacetylation rate (in this case consumption rate of NaOH) and substrate concentration (PVAc) is shown as filled markers in Figure 7.

Using solver utility in Excel for windows, values for parameters K_m and V_{max} were found by fitting eq 1 to the experimental data by least mean square regression fit. The left side of Figure 7 shows both the fitted and experimental data as solid lines and filled markers, respectively. The kinetic parameters K_m and V_{max} were input into eq 3 to solve for $1/V_0$ and the resulting data were used to generate the Lineweaver−Burk plots shown as solid lines on the right side of Figure 7. Experimental data for V_0 and substrate concentration were also used to generate the Lineweaver−Burk plots that are shown as filled markers on the right side of Figure 7. Linear regression analysis of this data and corresponding values of R^2 verify the linearity of experimental data. Furthermore, agreement between experimentally generated Lineweaver−Burk plots and corresponding fitted plots using data from eq 1 shows that deacetylation of PVAc, using HiC, PmC, and FsC, obeys Michaelis−Menten type kinetics.

In addition, by substituting V_{max} with $k_{cat}[E]_0$ from eq 2 into eq 1, and inputting experimental enzyme concentration values from Figure 6 where $[S]_0$ was fixed, eq 1 was used to generate V_0 (rate of NaOH consumption) values that are plotted in Figure 6 (dotted lines). As would be expected, the dotted line generated from eq 1 fits well with experimental results in the linear dependence region of $[E]_0$, where the Michaelis−Menten equation should be applicable.

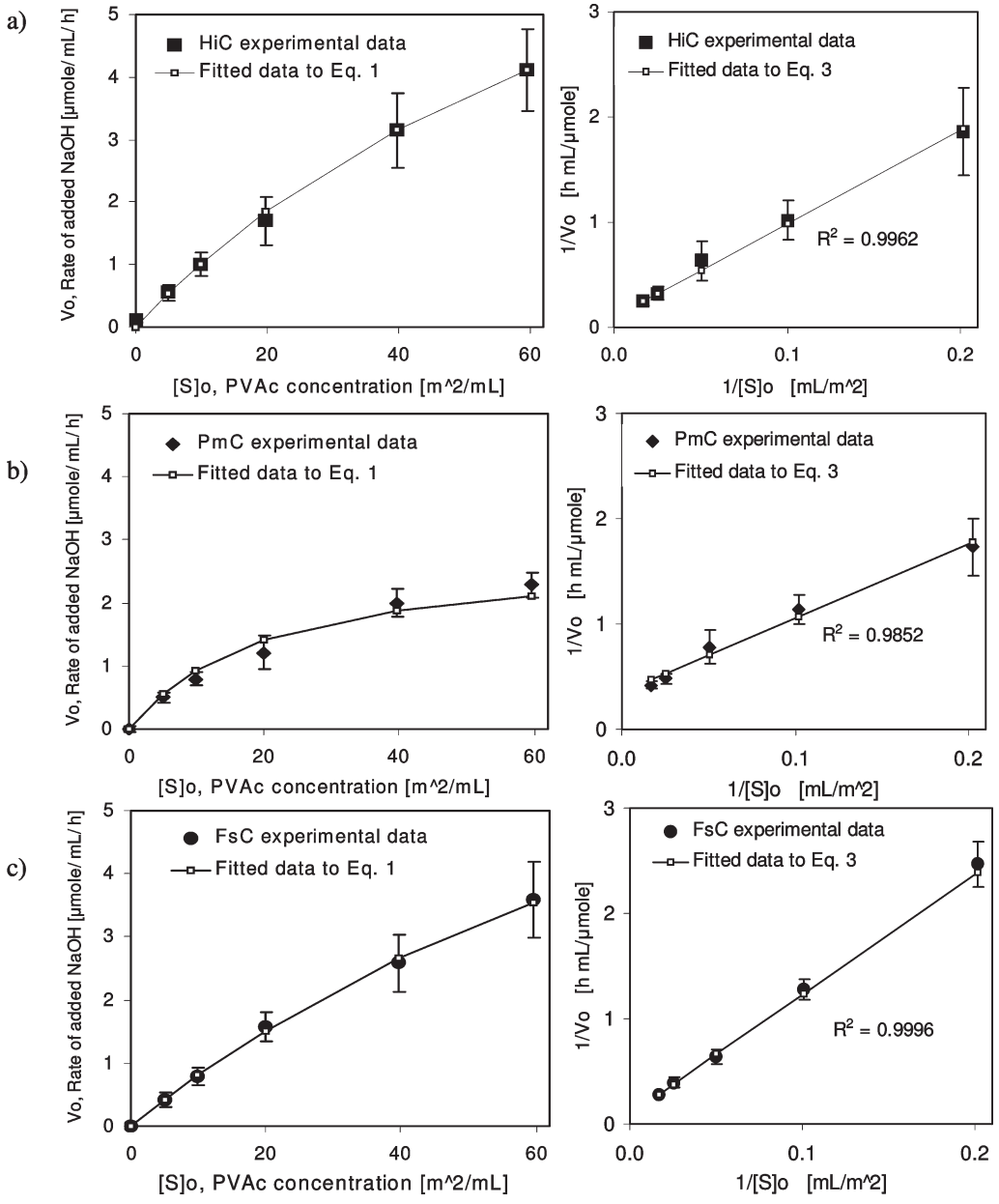

Figure 7. Initial rate of NaOH consumption as a function of the substrate concentration (PVAc) in the presence of (a) 1.0 nmol/mL HiC at 70 °C, (b) 2.0 nmol/mL PmC at 50 °C, and (c) 4.3 nmol/mL FsC at 40 °C. Experimental values are plotted as filled markers and the solid curves on the left- and right-hand sides are fitted to eq 1 and eq 3, respectively. Error bars represent standard deviation method based on duplicate repeats.

Table 1. Michaelis−Menten Parameters Determined for HiC, PmC, and FsC for PVAc Deacetylation at 70, 50, and 40 °C Respectively

	$[E]_0$ (nmol/mL)	K_m (m^2/mL)	V_{max} (μmol/(mL/h))	$k_{cat}/K_m = V_{max}/[E_0]/K_m$
HiC	1.1	94	11	102
PmC	4.3	20	3	75
FsC	2.0	125	11	20

Kinetic parameters reported in Table 1, determined by the M−M model for HiC, PmC, and FsC, are not intrinsic kinetic constants since the system studied is heterogeneous where it is difficult to account for interfacial properties, effects of mass transfer and other independent variables. Therefore, it is appropriate to consider Table 1 values as apparent kinetic values.[42] FsC possesses the lowest affinity for PVAc (high K_m value) and similar V_{max} values as HiC. In contrast, PmC has the highest affinity and lowest V_{max} values. To better compare the overall performance of the three cutinases, catalytic efficiency (k_{cat}/K_m), a relative value of the kinetic parameters that is independent of enzyme concentration, was calculated and listed in Table 1. HiC has the highest catalytic efficiency and would be the enzyme most susceptible to deacetylate PVAc. Though PmC has a low V_{max} value, its value of catalytic efficiency is larger than that of FsC, largely due to its higher substrate affinity.

The M−M kinetic model was originally proposed for homogeneous enzymatic reactions and is usually considered not applicable for heterogeneous systems.[43−51] Another kinetic model, proposed by Mukai et al.,[43] was developed to account for heterogeneity. The model predicts that, with increasing $[E]_0$, the rate of hydrolysis increases to a maximum and then starts decreasing at higher $[E]_0$, owing to surface overcrowding by the bound enzyme and, consequently, lack of free substrate at surfaces.[43,44] In work where this kinetic model was applied, polymer substrates were used in the form of films or micro particles with thicknesses or diameters

between 70 and 250 μm.[43−47] Observation of Figure 6 shows that, for PVAc distributed within S-DVB beads, a decrease in cutinase activity at higher enzyme concentrations was not observed. Therefore, the model by Mukai et al.[43] will not fit the experimental results obtained herein. By coating PVAc within a macroporous support, access of cutinases to substrate surfaces was greatly increased. Furthermore, the pore diameters within beads are sufficiently large to allow cutinases to move freely. Thus, by design, our system eases mass transfer and substrate access constraints moving closer to the behavior that would be observed where homogeneous kinetics is observed. Indeed, this may explain why the results obtained herein obey M−M kinetic behavior. Similarly, others who have designed systems to ease mass transfer and substrate access to enzymes have also successfully applied M−M kinetics to their results. For example, kinetics of cutinase-catalyzed reactions where the cutinase is immobilized on a macroporous support and a soluble substrate was used were successfully fit to M−M equations.[52,53] Furthermore, Chahinian et al.[28] applied the M−M model to study kinetic behavior of FsC for hydrolysis of vinyl acetate in emulsions, which also represents a heterogeneous enzyme−substrate system.

Thermostability Study of Cutinase-Catalyzed Deacetylation of PVAc. Kinetic and temperature studies were based on results from measured initial rates, determined during the first hour of cutinase−PVAc incubations. Also of interest is to determine whether HiC, PmC, and FsC can sustain their activities under optimized conditions during incubations conducted for extended times. Therefore, cutinases were incubated for up to 192 h (or 8 days) in 0.5 mM Tris at 70, 50, and 40 °C corresponding to optimal activity of HiC, PmC and FsC, respectively. As described in the experimental section, aliquots were withdrawn at predetermined times and assayed for activity using the pH-stat. Figure 8, illustrates the stability of the three cutinases as percentages of their initial activity before incubation (at $t = 0$). By 24, 48, and 96 h, FsC lost 14, 57, and 93% of its activity. PmC lost 41% of its activity within 48 h, but, thereafter, the remaining activity showed only small decreases so that, at 144 and 192 h, PmC retained 57 and 47% activity, respectively. Similarly, HiC lost 13% of its activity by 48 h, but thereafter, displayed good stability to 144 and 192 h where residual HiC activities are 80 and 67%, respectively. In contrast to the relatively poor stability found herein with FsC, Mantamá et al.[2] reported that FsC has a half-life of 134 days. Stability studies performed in Mantamá et al.[2] were conducted using similar glycerol concentrations in media. Furthermore, they performed experiments at 35 °C and pH 8.0, which is similar to conditions used herein (40 °C, pH 7.5). A noteworthy difference between FsC stability studies in ref 2 and herein is that, instead of using purified enzyme, Mantamá et al.[2] used a crude FsC preparation obtained directly from the culture broth of fermentative synthesis. Therefore, it could be that FsC was stabilized by a byproduct in culture media. Also, instead of assaying residual activity on the reaction of interest (acrylic−vinyl acetate fiber hydrolysis), Mantamá et al.[2] chose to use a surrogate assay, specifically *p*-nitrophenyl butyrate hydrolysis. It might be that alterations in enzymes during incubation have less effect on *p*-nitrophenyl butyrate hydrolysis then occurs for hydrolysis of VAc units along fibers.

Weight Loss of S-DVB/PVAc Beads and Products Formed. PVAc deacetylation is a polymer modification reaction that, potentially, can generate poly(VOH) chains if deacetylation is complete, or could form P(VAc-*co*-VOH) with various degrees of deacetylation. Indeed, cutinases may not be active

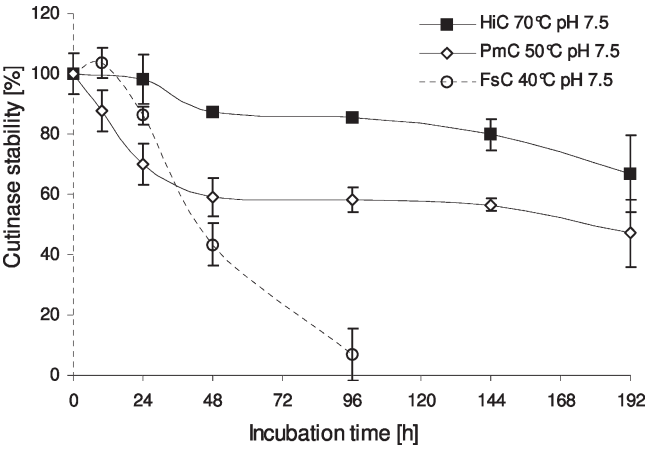

Figure 8. Thermal stability of HiC, PmC and FsC at 70, 50, and 40 °C, respectively, determined by monitoring initial activity on PVAc in S-DVB beads using 30 m^2/mL PVAc in 0.5 mM Tris−HCl buffer with 10% glycerol at pH 7.5 with 15 μM of either HiC, PmC, or FsC. Error bars represent standard deviation method based on duplicate repeats.

on chains that are partially deacetylated or may have selectivity during deacetylation giving P(VAc-*co*-VOH) with specific sequence distributions. For example, cutinases might only hydrolyze every other VAc unit giving an alternating copolymer. If certain degrees of hydrolysis are achieved along copolymer chains, water-soluble products will be formed that will diffuse into incubation media from surfaces of S-DVB beads. Alternatively, if deacetylation along chains occurs to low extents, then P(VAc-*co*-VOH) products will remain insoluble along surfaces within S-DVB beads. Figure 9 shows weight loss of S-DVB beads coated with PVAc as a function of cutinase used and incubation time. The weigh-tloss is expressed as a percentage of the initial weight of PVAc which constitutes 43%-by-wt of the coated S-DVB beads. It is assumed that the weight loss is only due to hydrolysis of PVAc and not to any loss of S-DVB. As predicted from the kinetic study, HiC is most susceptible to deacetylate PVAc resulting in 16% weight loss at 144 h. In contrast, incubations of PVAc coated S-DVB beads with FsC resulted in the lowest weight loss, up to 2% weight loss by 48 h, with no further weight loss as incubations were continued to 96 h. The fact that weight loss reaches a maximum value after only 48 h is consistent with the rapid loss in FsC activity during incubations (see Figure 8) such that, by 48 h FsC retained 40% of its original activity. Furthermore, FsC showed the lowest catalytic efficiency (Table 1) of the three cutinases studied. Thus, even though the M−M kinetic model does not take enzymatic stability into account, the catalytic efficiency parameter determined by an M−M kinetic analysis correctly predicted the relative performance of the three cutinases during long-term incubations. In addition, study of Figure 8 shows that the loss in activity for PmC during incubations for 48, and up to 192 h, was far less severe than was observed for FsC. Hence, PmC thermal stability does not provide an adequate explanation for that, beyond 48 h incubations, PmC did not catalyze further weight loss of PVAc-coated S-DVB beads (Figure 9).

The question posed above is as follows: what is the composition of polymer products formed by cutinase-catalyzed PVAc hydrolysis? Poly(VAc-*co*-VOH), consisting of VAc and VOH units, can have three different dyad sequences: (VAc−VAc), (VOH−VAc), and (VOH−VOH). A similar notation is used for the six different types of triad sequences. ^{1}H NMR was used to analyze the composition and sequence distribution of formed products dissolved in

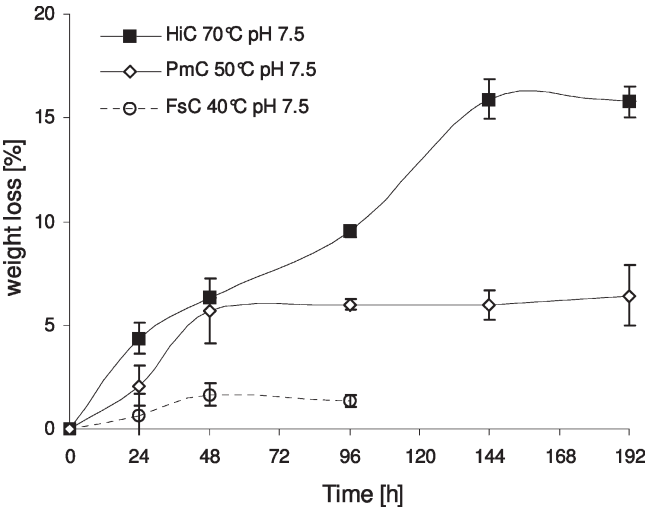

Figure 9. Weight loss of PVAc (30 m^2/ml) coated within S-DVB beads as a function of reaction time in 1 M Tris−HCl with 10% glycerol, at pH 7.5, and with 15 μM of either HiC, PmC or FsC at 70, 50, or 40 °C respectively. Error bars represent the standard deviation method based on triplicate repeats.

DSMO-d_6, which is a good solvent for both PVAc and PVOH.[54−56] Figure 10 shows an example of a ^{1}H NMR spectrum recorded on water-soluble poly(VAc-*co*-VOH) formed during an incubation of PVAc with HiC for 144 h. Peak assignments, displayed in Figure 10, were made based on previously published NMR studies on poly(VAc-*co*-VOH).[54,56] Methylene proton resonances are broad peaks at 1.75, 1.58, and 1.43 ppm, which are ascribed to the dyads (VAc−VAc), (VOH−VAc), and (VOH−VOH), respectively. Methyl proton resonances of VAc units are found from 1.87-to-1.97 ppm, depending on composition and configuration of sequences.[54,57] Methine protons give rise to six different resonances, which are assigned to six compositional triads. Thus, resonances of (VOH−VAc−VOH), (VAc−VAc−VOH) and (VAc−VAc−VAc) are located at 5.10, 4.96, and 4.80 ppm, respectively. Also, (VOH−VOH−VOH), (VAc−VOH−VOH), and (VAc−VOH−VAc) are found at lower chemical shifts, specifically 3.85, 3.65, and 3.45 ppm, respectively. In the region 4.10−4.52 ppm, resonances are due to hydroxyl protons of the copolymer.[54]

Weight loss studies using FsC and PmC gave maximum yields of water-soluble P(VAc-*co*-VOH) of 2−5%, or 6−15 mg from 6 mL of incubation media (see Figure 9). At this reaction scale it is difficult to recover sufficient quantities of purified copolymers for NMR analysis. Experiments were not scaled-up due to limited availability of purified cutinases. Hence, for this study, analysis of water-soluble P(VAc-*co*-VOH) focused on experiments with HiC, where highest yields were obtained. Copolymer compositions were determined from the relative intensities of methyl and methylene proton resonances between 1.87 and 1.97 ppm and 1.43−1.75 ppm, respectively, as reported by van der Velden and Beulen.[54] The mol fraction of VAc in P(VAc-*co*-VOH), solubilized during incubations for 24, 144, and 192 h with HiC (70 °C, pH 7.5), is 0.30 ± 0.09, 0.19 ± 0.02, and 0.06 ± 0.02, respectively. Correspondingly, yields of water-soluble copolymer after incubations with HiC for 144 and 192 h are 13% and 14%, respectively. The yields represent the weight of recovered water-soluble polymer relative to the weight of PVAc within beads at time 0. The yields of water-soluble P(VAc-*co*-VOH) correspond well with the weight loss, illustrated in Figure 9. The observed decrease in VAc content in water-soluble copolymers with increased incubation time, or the increase in P(VAc-*co*-VOH) deacetylation, suggests that HiC not only deacetylates PVAc adsorbed on S-DVB forming newly solubilized P(VAc-*co*-VOH) chains but also continues to hydrolyze VAc units of water-soluble P(VAc-*co*-VOH) that has been in media for variable times. It may be that the heterogeneity of VAc contents of water-soluble P(VAc-*co*-VOH) is extreme due to variable residence times of chains in aqueous media. Between 144 and 192 h, where no further weight loss of PVAc was observed (Figure 9), the deacetylation of water-soluble P(VAc-*co*-VOH) chains progresses so that, by 192 h, only 6 mol % of VAc units remain. This demonstrates that HiC is active for deacetylation of P(VAc-*co*-VOH) with highly variable VAc contents. In other words, HiC can deacetylate P(VAc-*co*-VOH) with very different levels of hydrophobicity. The fact that no further weight loss of PVAc coated S-DVB beads was observed after 144 h (Figure 9) was unexpected given that HiC remained active for 192 h incubations under identical conditions, but without substrate (Figure 8). One explanation is that, HiC may have a higher affinity for P(VAc-*co*-VOH) dissolved in media than absorbed on S-DVB, If so, lower concentrations of HiC within S-DVB beads would lead to decreased degradation of water-insoluble adsorbed substrate. Additional experiments will be required using water-soluble P(VAc-*co*-VOH) to better understand the activity of cutinases on these substrates as well as the extent that P(VAc-*co*-VOH) could function as an inhibitor.

The properties P(VAc-*co*-VOH), such as hydrophobicity, solubility, and degree of crystallinity are more strongly dependent on the degree of hydrolysis. However, these properties are also dependent on the sequence distribution of VAc and VOH units along P(VAc-*co*-VOH) chains. The sequence distribution is generally characterized by

$$\eta = \frac{(\mathrm{VAc-VOH})}{2(\mathrm{VOH})(\mathrm{VAc})} \quad (4)$$

where η is a measure of departure from random character. Relationship between values of η and sequence distribution are as follows: $0 \leq \eta > 1$ for blockier distributions; $\eta = 0$ for block copolymers; $\eta = 1$ for completely random cases; $1 < \eta \geq 2$ for alternate−like cases.[37,56] It is well-known that, by varying the chemical route to P(VAc-*co*-VOH) copolymers, different sequence distributions can be attained.[37,56] By reacetylation of PVOH, copolymers with random distribution ($0.8 < \eta > 1.1$) are prepared. In contrast, hydrolysis of PVAc by acidification results in block-like sequence copolymers ($0.5 < \eta > 0.8$). Copolymers with higher block-like character ($0.4 < \eta > 0.5$) are prepared by direct saponification of PVAc.[37,56] Within the first 24 h of HiC catalyzed hydrolysis of PVAc, where the enzyme is mainly hydrolyzing the water-insoluble PVAc coated on S-DVB (because the water-soluble fraction is of merely 6% yield), the sequence distribution of the formed water-soluble P(VAc-*co*-VOH) is highly blocky with $\eta = 0.36 \pm 0.06$, a comparable value to that of the saponification method. This result suggests that adsorption of the enzyme might occur so that the active site is positioned to hydrolyze acetyl groups with neighboring VOH units. As the incubation time progresses to 144 h, the isolated water-soluble copolymer has only 6 mol % VAc units. Characterization of products becomes increasingly complex since water-soluble copolymers formed earlier during incubations have been exposed to HiC in the aqueous media for long periods of time. Concurrently, HiC has access to PVAc chains adsorbed on S-DVB beads and can form new water-soluble chains with lower residence times in the aqueous phase. Furthermore, at

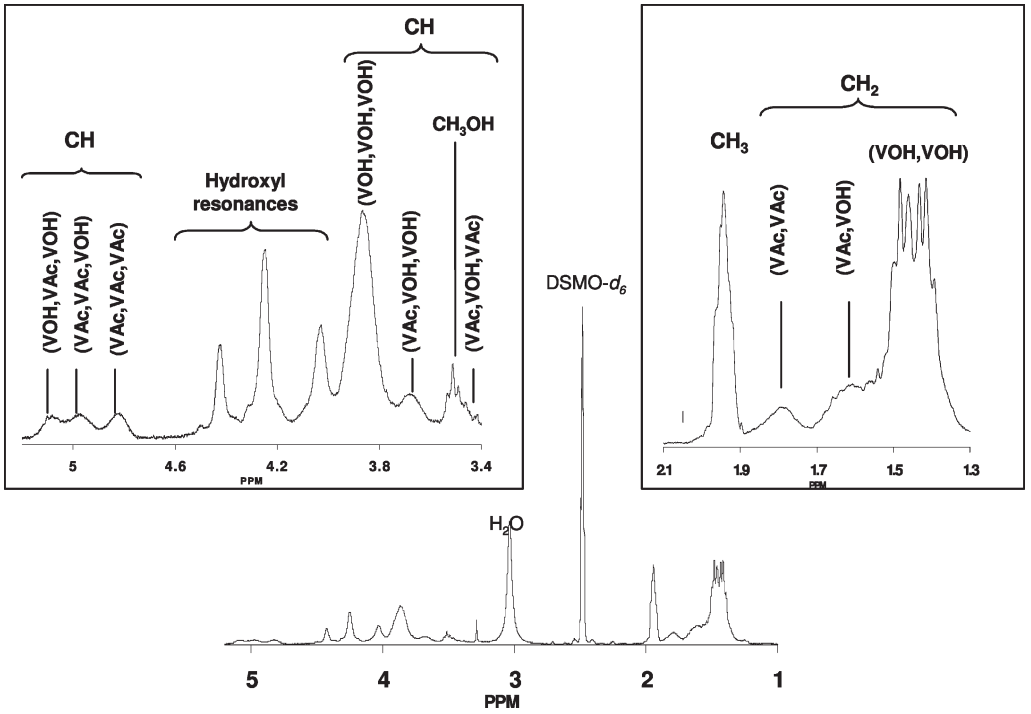

Figure 10. ^{1}H NMR spectrum (300 MHz, in DSMO-d_6 at 70 °C) of water-soluble P(VAc-*co*-VOH) formed during a 144 h incubation with HiC along with expansions of spectral regions from 3.4 to 5.2 ppm and 1.3−2.1 ppm.

such a high conversion of acetate units to VOH units, the reaction is no longer under kinetic control and the distribution of repeat units is likely dictated by thermodynamics. Hence, the sequence observed tends toward a random distribution ($\eta = 0.68 \pm 0.08$).

Conclusions

This paper compares the activity of three different cutinases in purified form, notably HiC, PmC and FsC, for deacetylation of PVAc. Their initial activities were successfully fitted to the M-M kinetic model at their optimized temperatures. The resulting kinetic parameters gave experimentally determined values of substrate-enzyme affinity, maximal reaction rate and catalytic efficiency. Comparison of these values provides a basis to understand on a molecular level differences in their activities. The kinetic model correctly predicted the relative performance of the three cutinases when incubated with PVAc coated on S-DVB beads for extended incubation times. HiC has its optimal initial activity at the highest temperature (70 °C) and also showed highest catalytic efficiency and thermostability. These characteristics enabled HiC to attain the largest extents of PVAc deacetylation during extended incubations with PVAc coated on S-DVB beads. In contrast, FsC displayed the poorest affinity toward PVAc, lowest catalytic efficiency and worst thermo stability (lost 93% of its activity within 96 h at 40 °C). This explains why FsC showed the lowest degree of PVAc degradation, only 2% weight loss during a 96 h incubation. HiC-catalyzed degradation of PVAc formed up to 14% by weight of a deacetylated P(VAc-*co*-VOH) fraction that was soluble in the aqueous media. As HiC hydrolysis of PVAc progressed with time, almost pure PVOH (94% hydrolyzed) was formed. The results reported herein support further development of cutinases as valuable catalysts that can be used to remove PVAc from various surfaces or composites. Furthermore, cutinase-catalyzed PVAc hydrolysis provides an environmentally friendly alternative to saponification for the production of PVOH with varying degree of hydrolysis.

Acknowledgment. We thank the National Science Foundation Industry/ University Cooperative Research Center (NSF-I/UCRC) for Biocatalysis and Bioprocessing of Macromolecules at Polytechnic University for their financial support, intellectual input, and encouragement during the course of this research. We are also grateful to Dr. Lisa Miller and colleagues for providing access to the FTIR facilities at the National Synchrotron Light Source (Brookhaven National Laboratory, Upton, New York 11973).

Supporting Information Available: Figures showing lots of NaOH titrated versus time for pH-stat studies as a function of temperature (Figure S-1), cutinase concentration (Figure S-2), and substrate concentration (Figure S-3). This material is available free of charge via the Internet at http://pubs.acs.org.

References and Notes

(1) Borch, K.; Lund, H.; Sharyo, M.; Sakaguchi, H.; Pedersen, H.; Fitzhenry, J. F. Enzymatic hydrolysis of a polymer comprising vinyl acetate monomer. US 2004/0226672 A1, May 14 **2004**.
(2) Matamá, T.; Vaz, F.; Gubitz, G. M.; Cavaco-Paulo, A. *Biotechnol. J.* **2006**, *1*, 842–849.
(3) Park, J. W.; Im, S. S. *Polymer* **2003**, *44*, 4341–4354.
(4) Sivalingam, G.; Chattopadhyay, S.; Madras, G. *Chem. Eng. Sci.* **2003**, *58*, 2911–2919.
(5) Abou-Aiad, T. H.; El-Sabee, M. Z.; Abd-El-Nour, K. N.; Saad, G. R.; A, E.-S.; Gaafar, E. A. *J. Appl. Polym. Sci.* **2002**, *86*, 2363–2374.
(6) Nuttelman, C. R.; Henry, S. M.; Anseth, K. S. *Biomaterials* **2002**, *23*, 3617–3626.
(7) Darwis, D.; Stasica, P.; Razzak, M. T.; Rosiak, J. M. *Radiat. Phys. Chem.* **2002**, *63*, 539–542.
(8) Zhang, F.; McGinity, J. W. *Drug Dev. Ind. Pharm.* **2000**, *26*, 931–942.
(9) Gonzalez, G. A.; Novoaa, J. H.; Mirzab, S.; Antikainenb, O.; Colartea, A. I.; Pazd, A. S.; Yliruusi, J. *Eur. J. Pharm. Biopharm.* **2005**, *59*, 343–350.
(10) Palamara, J. E.; Zielinski, J. M.; Hamedi, M.; Duda, J. L.; Danner, R. P. *Macromolecules* **2004**, *37*, 6189–6196.
(11) Guebitz, G.; Cavaco-Paulo, A. *Trends Biotechnol.* **2007**, *26* (1), 32–38.
(12) Kolattukudy, P. E. *Science* **1980**, *208*, 990–1000.

(13) Kolattukudy, P. E. Cutinase from fungi and pollen. In *Lipases*; Borgstrom, B., Brockman, H. L.; Elsevier: Amsterdam, 1984; Vol. *18*, pp 471−504.
(14) Ettinger, W. F.; Thukral, S. K.; Kolattukudy, P. E. *Biochemistry* **1987**, *26*, 7883–7892.
(15) Longhi, S.; Cambillau, C. *Biochim. Biophys. Acta* **1999**, *1441*, 185–196.
(16) Egmond, M. R.; de Vlieg, J. *Biochimie* **2000**, *82*, 1015–1021.
(17) Carvalho, C. M. L.; Aires-Barros, M. R.; Cabral, J. M. S. *J. Biotechnol.* **1998**, *1* (3), 160–171.
(18) Mannesse, M. L.; Cox, R. C.; Koops, B. H.; Verheij, H. M.; de Haas, G. H.; Egmond, M. R.; van der Hijden, H. T. W. M.; de Vlieg, J. *Biochemistry* **1995**, *34*, 6400–6407.
(19) Nicolas, A.; Egmond, M. R.; Verrips, T.; de Vlieg, J.; Longhi, S.; Cambillau, C.; Martinez, C. *Biochemistry* **1996**, *35*, 398–410.
(20) Alisch, M.; Feuerhack, A.; Muller, H.; Mensak, B.; Andreaus, J.; Zimmermann, W. *Biocatal. Biotransform.* **2004**, *22*, 347–351.
(21) Eberl, A.; Heumann, S.; Kotek, R.; Kaufmann, F.; Mitsche, S.; Cavaco-Paulo, A.; Gubitz, G. M. *J. Biotechnol.* **2008**, *135*, 45–51.
(22) Heumann, S.; Eberl, A.; Pobeheim, H.; Liebminger, S.; Fischer-Colbrie, G.; Almansa, E.; Cavaco-Paulo, A.; Gubitz, G. M. *J. Biochem. Biophys. Methods* **2006**, *39*, 89–99.
(23) Yoon, M. Y.; Kellis, J. T.; Poulouse, A. J. *AATCC Rev.* **2002**, *2* (6), 33–36.
(24) Ivanova, T.; Malzert, A.; Boury, F.; Proust, J. E.; Verger, R.; Panaiotov, I. *Colloids Surf. B: Biointerfaces* **2003**, *32*, 307–320.
(25) Silva, C.; Matamá, T.; Gubitz, G. M.; Cavaco-Paulo, A. *J. Polym. Sci.* **2005**, *43*, 2749–2753.
(26) Vertommen, M. A. M. E.; Nierstrasz, V. A.; van der Veer, M.; Warmoeskerken, M. M. C. G. *J. Biotechnol.* **2005**, *120*, 376–386.
(27) Silva, C.; Carneiro, F.; O'Neill, A.; Fonseca, L. P.; Cabral, J. M. S.; Guebitz, G.; Cavaco-Paulo, A. *J. Polym. Sci.* **2005**, *43*, 2448–2450.
(28) Chahinian, H.; Nini, L.; Boitard, E.; Dubes, J.-P.; Comeau, L.-C.; Sarda, L. *Lipids* **2002**, *37*, 653–662.
(29) Tolner, B.; Smith, L.; Begent, R. H. J.; Chester, K. A. *Nat. Protocols* **2006**, *1* (2), 1006–1023.
(30) Mei, Y.; Miller, L.; Gao, W.; Gross, R. A. *Biomacromolecules* **2003**, *4*, 70–74.
(31) Chen, B.; Miller, E.; Miller, L.; Maikner, J.; Gross, R. A. *Langmuir* **2007**, *23*, 1381–1387.
(32) Gebauer, B.; Jendrossek, D. *Appl. Environ. Microbiol.* **2006**, *72*, 6094–6100.
(33) Chang, B.; Larson, E.; Whitman-Guliaev, C. *Bioradiations* **2005**, *115*, 17–23.
(34) Calado, C. R. C.; Taipa, M. A.; Cabral, J. M. S.; Fonseca, L. P. *Enzyme Microbiol. Technol.* **2002**, *31*, 161–170.
(35) Nielsen, A. D.; Arleth, L.; Westh, P. *Langmuir* **2005**, *21*, 4299–4307.
(36) Sebastian, J. *Arc. Biochem. Biophys.* **1988**, *263* (2), 77–85.
(37) Isasi, J. R.; Cesteros, L. C.; Katime, I. *Macromolecules* **1994**, *27*, 2200–2205.
(38) Martinez, C.; Geus, P.; Lauwereys, M.; Cambillau, C. *Nature* **1992**, *356*, 615–618.
(39) Petersen, S.; Fojan, P.; Petersen, E. I.; Neves Petersen, M. T. *J. Biomed. Biotechnology* **2001**, *1* (2), 62–69.
(40) Boyer, R. F. Kinetic analysis of tyrosinase. In *Modern experimental biochemistry*, 3rd ed.; Cummings, B., Eds; Elsevier: San Francisco, CA, 2000; pp 279−299.
(41) Bommarius, A. S.; Riebel, B. R. *Biocatalysis Fundamentals and Applications*; Wiley-VCH: Weinheim, Germany, 2004; p 611.
(42) Carvalho, C. M. L.; Aires-Barros, M. R.; Cabral, J. M. S. *J. Biotechnol.* **2000**, *81*, 1–13.
(43) Mukai, K.; Yamada, K.; Doi, Y. *Int. J. Biol. Macromol.* **1993**, *15*, 361–366.
(44) Timmins, M. R.; Lenz, R. W. *Polymer* **1997**, *38*, 551–562.
(45) Wu, C.; Jim, T. F.; Gan, Z.; Zhao, Y.; Wang, S. *Polymer* **2000**, *41*, 3593–3597.
(46) Kasuya, K.; Inoue, Y. *Polym. Degrad. Stab.* **1995**, *48*, 167–174.
(47) Spyros, A.; Kimmich, R. *Macromolecules* **1997**, *30*, 8218–8225.
(48) McLaren, A. D. *Enzymologia* **1963**, *26*, 237–246.
(49) Figueroa, Y.; Hinks, D.; Montero, G. *Biotechnol. Prog.* **2006**, *22*, 1209–1214.
(50) Xu, F.; Ding, H. *Appl. Catal.* **2007**, *317*, 70–81.
(51) Scandola, M.; Focarete, M. L.; Frisoni, G. *Macromolecules* **1998**, *31*, 3849–3851.
(52) Goncalves, A. P. V.; Cabral, J. M. S.; Aires-Barros, M. R. *Appl. Biochem. Biotechnol.* **1995**, *60*, 217–228.
(53) Goncalves, A. P. V.; Lopes, J. M.; Lemos, F.; Ramoa Ribeiro, F.; Praceres, D. M. F.; Cabral, J. M. S.; Aires-Barros, M. R. *Enzyme Microb. Technol.* **1997**, *20*, 93–101.
(54) van der Velden, G.; Beulen, J. *Macromolecules* **1982**, *15*, 1071–1075.
(55) Wu, T. K.; Ovenall, D. W. *Macromolecules* **1974**, *7*, 776–779.
(56) Moritani, T.; Fujiwara, Y. *Macromolecules* **1977**, *10*, 532–535.
(57) Moritani, T.; Kuruma, I.; Shibatani, K.; Fujiwara, Y. *Macromolecules* **1972**, *5*, 577–580.